

**RAPID MACROCELL TESTS OF
2205 AND XM-28 REINFORCING BARS**

By

Matthew O'Reilly

David Darwin

A Report on Research Sponsored by the

**NEW YORK STATE
DEPARTMENT OF TRANSPORTATION**

**Structural Engineering and Engineering Materials
SL Report 13-2a**

**THE UNIVERSITY OF KANSAS CENTER FOR RESEARCH, INC.
LAWRENCE, KANSAS
January 2013**

ABSTRACT

The corrosion resistance of 2205 and XM-28 stainless steel bars from two producers and provided by a single supplier was tested in accordance with Annexes A1 and A2 of ASTM 955-12. Three heats of stainless steel were tested: XM-28 stainless steel from producer A, 2205 stainless steel from producer B, and XM-28 stainless steel, also from producer B. The bars from producer A were supplied in two conditions, as cut from the coil and after having been straightened, while the bars supplied by producer B were rolled straight. The XM-28 stainless steel bars satisfied the requirements specified in Annexes A1 and A2 of ASTM 955. The 2205 stainless steel bars did not satisfy the requirements specified in Annexes A1 and A2 of ASTM 955, exhibiting individual corrosion rates greater than 0.50 $\mu\text{m}/\text{yr}$ and an average corrosion rate greater than 0.25 $\mu\text{m}/\text{yr}$. The process of straightening coiled stainless steel reinforcement damages the transverse deformations of the bars and can leave deposits, either of which can serve as initiation sites for corrosion.

Keywords: chlorides, concrete, corrosion, macrocell, reinforcing steel, stainless steel

INTRODUCTION

This report describes the test procedures and results of rapid macrocell tests to evaluate the corrosion performance of 2205 and XM-28 stainless steel reinforcing bars before and after straightening. The tests were performed on No. 5 (No. 16) stainless steel bars from a single supplier. Three heats of stainless steel were tested: XM-28 stainless steel from producer A, 2205 stainless steel from producer B, and XM-28 stainless steel, also from producer B. The bars from producer A were supplied in two conditions, as cut from the coil and after having been straightened, while the bars supplied by producer B were rolled straight. For each type of steel, six specimens are tested in accordance with Annexes A1 and A2 of ASTM A955.

EXPERIMENTAL WORK

Materials

The chemical compositions of the bars are presented in Table 1.

The straightened bars from producer A had damage to the transverse deformations from the straightening process (Figure 1a). The coiled bars had less damage to the transverse deformations, but still showed some flattening of the deformations (Figure 1b). The 2205 bars from producer B had a mottled appearance (Figure 2). No other damage and no corrosion products were noted on any of the reinforcement. Past results suggest that bars like the 2205 bars from producer B that do not have a bright or uniformly light surface finish do not perform well.

Table 1: Chemical composition of stainless steels

Steel(Producer)	Heat	Chemical Analysis, %										
		C	Co	Cr	Cu	Mn	Mo	N	Ni	P	S	Si
XM-28(A)	B0J3	0.045	-	16.79	-	12.34	-	0.302	0.74	0.034	0.0016	0.33
XM-28(B)	153480	0.05	0.06	17.47	0.08	12.04	0.12	0.32	0.73	0.019	0.001	0.33
2205(B)	153101	0.02	-	21.22	0.23	1.70	2.57	0.17	4.83	0.024	0.004	0.45



Figure 1a: Damage to deformations on straightened XM-28 bars from the straightening process.



Figure 1b: Damage to deformations on coiled XM-28 bars.



Figure 2: 2205 as-received.

Experimental Procedures

For each type of stainless steel and condition (coiled, straightened, or straight), six specimens are tested in accordance with the rapid macrocell test outlined in Annexes A1 and A2 of ASTM A955/A955M-10 and detailed in Figure 3. Bars used in the rapid macrocell test are 5 in. long and drilled and tapped at one end to accept a 0.5-in., 10-24, stainless steel machine screw. Bars are wiped with acetone prior to testing to remove oil and surface contaminants introduced by machining or handling. A length of 16-gauge insulated copper wire is attached to each bar using the stainless steel screw. The electrical connection is coated with epoxy to protect the wire from corrosion.

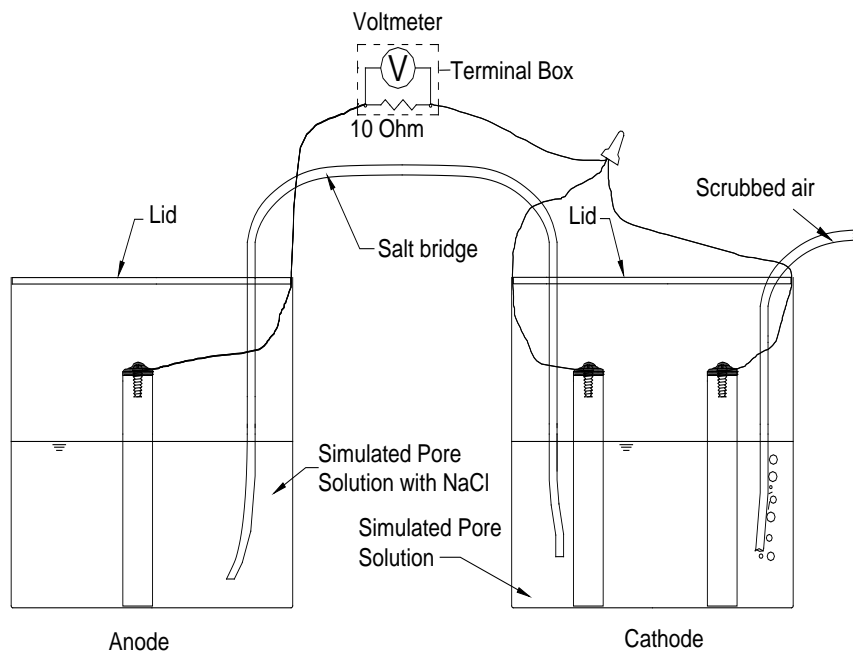


Figure 3: Rapid Macrocell Test Setup

A single rapid macrocell specimen consists of an anode and a cathode. The cathode consists of two bars submerged to a depth of 3 in. in simulated concrete pore solution in a plastic container, as shown in Figure 3. One liter of pore solution consists of 974.8 g of distilled water, 18.81 g of potassium hydroxide (KOH), and 17.87 g of sodium hydroxide (NaOH). Air, scrubbed to remove carbon dioxide, is bubbled into the cathode solution. The anode consists of a single bar submerged in a solution consisting of simulated pore solution and 15 percent sodium chloride (NaCl).

The solution at the anode is prepared by adding 172.1 g of NaCl to one liter of pore solution. The solutions are changed every five weeks to limit the effects of carbonation. The anode and cathode are connected electrically across a 10-ohm resistor. A potassium chloride (KCl) salt bridge provides an ionic connection between the anode and the cathode (Figure 3).

The corrosion rate is calculated based on the voltage drop across the 10-ohm resistor using Faraday's equation.

$$\text{Rate} = K \frac{V \cdot m}{n \cdot F \cdot D \cdot R \cdot A} \quad (1)$$

where the Rate is given in $\mu\text{m}/\text{yr}$, and

K = conversion factor = $31.5 \cdot 10^4 \text{ amp} \cdot \mu\text{m} \cdot \text{sec} / \mu\text{A} \cdot \text{cm} \cdot \text{yr}$

V = measured voltage drop across resistor, millivolts

m = atomic weight of the metal (for iron, $m = 55.8 \text{ g/g-atom}$)

n = number of ion equivalents exchanged (for iron, $n = 2$ equivalents)

F = Faraday's constant = 96485 coulombs/equivalent

D = density of the metal, g/cm^3 (for iron, $D = 7.87 \text{ g}/\text{cm}^3$)

R = resistance of resistor, ohms = 10 ohms for the test

A = surface area of anode exposed to solution, 39.9 cm^2

Using the values listed above, the corrosion rate simplifies to:

$$\text{Rate} = 29.0V \quad (2)$$

To satisfy ASTM A955, no individual reading may exceed $0.50 \text{ }\mu\text{m/yr}$ and the average corrosion rate of all specimens may not exceed $0.25 \text{ }\mu\text{m/yr}$ at any time during the 15-week test. In both cases, the corrosion current must be such as to indicate net corrosion at the anode. Current indicating a “negative” value of corrosion, independent of value, does not indicate corrosion of the anode and is caused by minor differences in oxidation rate between the single anode bar and the two cathode bars.

In addition to the corrosion rate, the corrosion potential is measured at the anode and cathode using a saturated calomel electrode (SCE). Readings are taken daily for the first week and weekly thereafter.

Results

The average corrosion rates for the XM-28 and 2205 stainless steels are shown in Figure 4. The highest average corrosion rate observed, $0.80 \text{ }\mu\text{m/yr}$ – above the ASTM A955 maximum of $0.25 \text{ }\mu\text{m/yr}$ – occurred on week 15 for the 2205 stainless steel from producer B. The average corrosion rate for the 2205 bars exceeded $0.25 \text{ }\mu\text{m/yr}$ at weeks 9, 10, 13, and 14. The coiled XM-28 (XM-28c) and straightened XM-28 (XM-28s) bars from producer A exhibited average corrosion rates of less than $0.1 \text{ }\mu\text{m/yr}$ throughout the test. The average corrosion rate for XM-28 from producer B never exceeded $0.02 \text{ }\mu\text{m/yr}$. No coiled or straightened XM-28 bar had an average corrosion rate exceeding the $0.25 \text{ }\mu\text{m/yr}$ limit specified by ASTM A955.

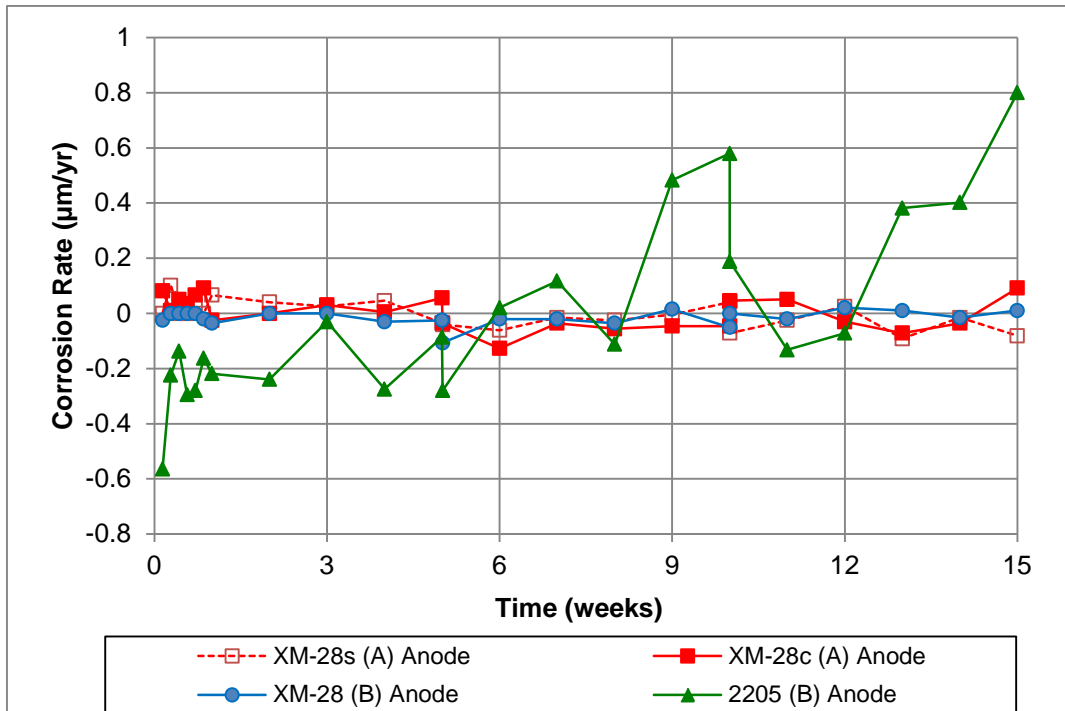


Figure 4: Average corrosion rates ($\mu\text{m}/\text{yr}$) for coiled and straightened XM-28 and 2205 stainless steel.

The individual corrosion rates for the coiled and straightened XM-28 stainless steel bars from producer A are shown in Figures 5a and 5b, respectively. For XM-28c (Figure 5a), the peak corrosion rate was $0.49 \mu\text{m}/\text{yr}$ and occurred in specimen 5 on day 4. Five of the six specimens had a positive corrosion rate at some point during the test, but no specimen exceeded the $0.50 \mu\text{m}/\text{yr}$ threshold set in ASTM A955. For XM-28s (Figure 5b), the peak corrosion rate was $0.49 \mu\text{m}/\text{yr}$ in specimen 6 at week 5, after the solution change. All six specimens had a positive corrosion rate at some point during the test, but no specimen exceeded the $0.50 \mu\text{m}/\text{yr}$ threshold set in ASTM A955.

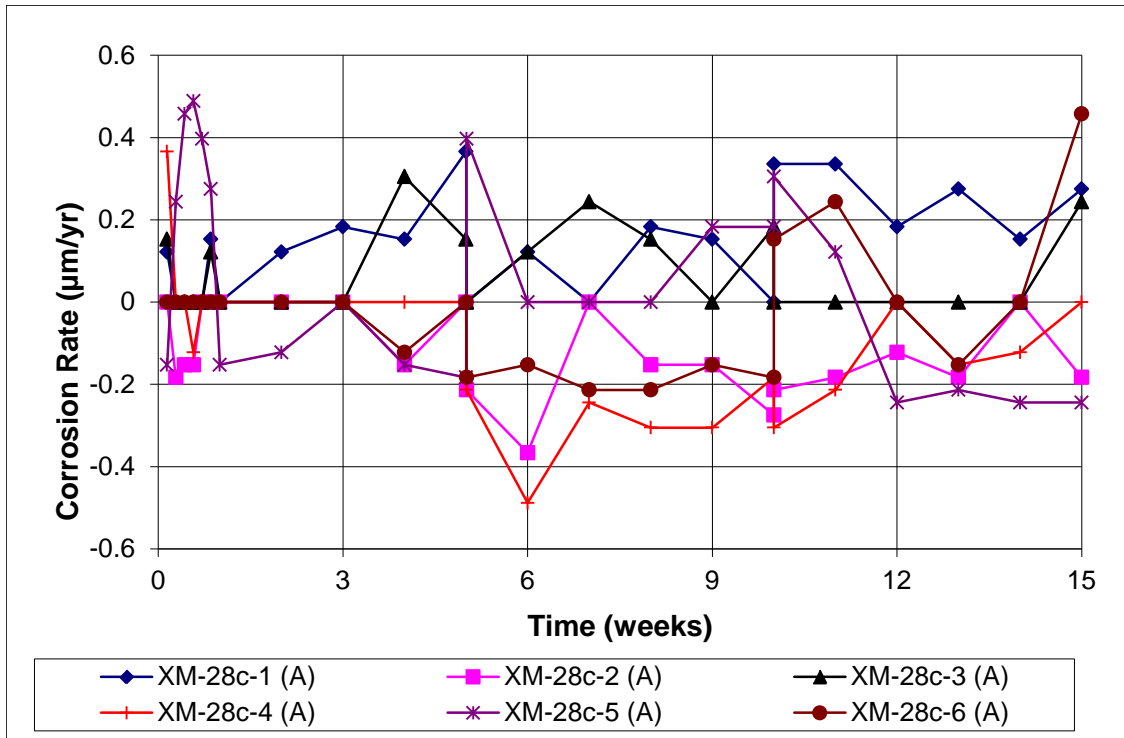


Figure 5a: Individual corrosion rates ($\mu\text{m}/\text{yr}$) for coiled XM-28 stainless steel from producer A.

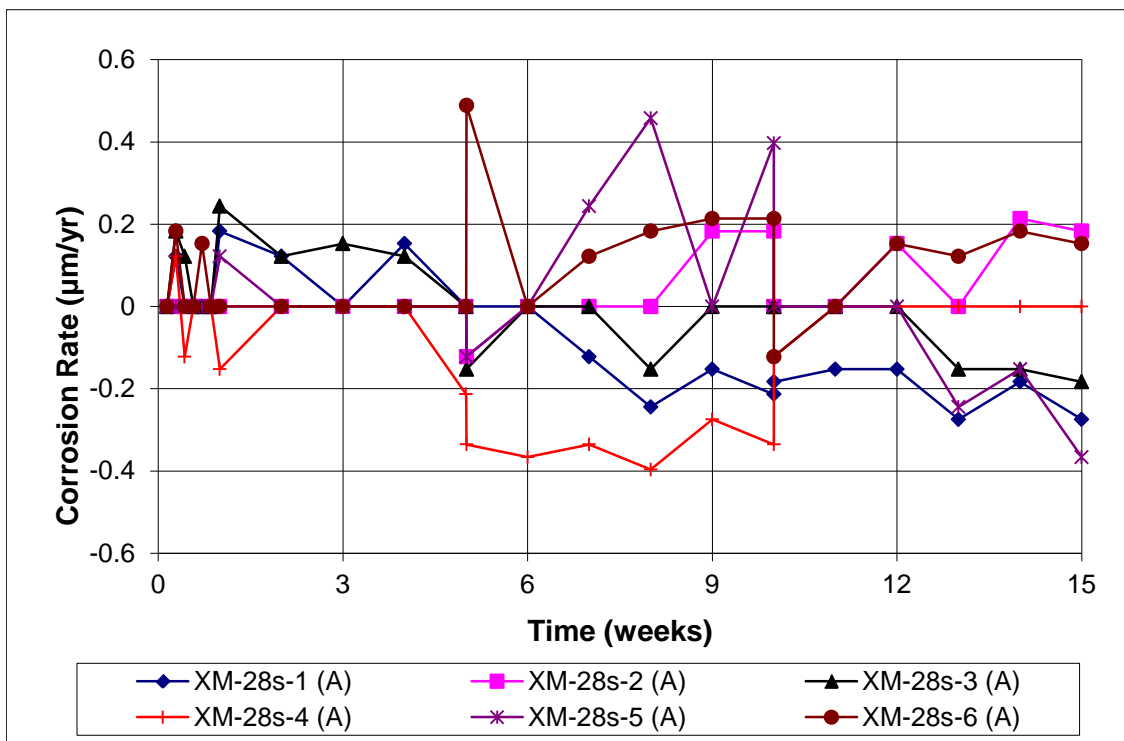


Figure 5b: Individual corrosion rates ($\mu\text{m}/\text{yr}$) for straightened XM-28 stainless steel from producer A.

Individual corrosion potentials at the anode are shown in Figures 6a and 6b for, respectively, the coiled and straightened XM-28 bars from producer A. The individual cathode corrosion potentials are shown in Figures 7a and 7b. Average potentials are shown in Figure 8. Both the coiled (Figure 6a) and the straightened (Figure 6b) XM-28 bars had potentials between -0.23 V and -0.26 V at the start of testing. For most specimens, the corrosion potentials became less negative over time and approached -0.15 V. ASTM C876 states a corrosion potential more negative than -0.275 V with respect to a calomel electrode (-0.350 V with respect to a copper sulfate electrode) indicates a greater than 90 percent probability of active corrosion for conventional steel, suggesting the steel in this test remained passive. The potential for specimen XM-28c-5 (A) dropped to around -0.30 V for several days during the first week of testing and at week 10 (Figure 6a), corresponding with an increase in corrosion rate (Figure 5a). The corrosion potential was otherwise comparable with the other specimens. The potential for specimen XM-28c-6 (A) dropped to around -0.23 V at week 15, also corresponding with an increase in corrosion rate (Figure 5a). Specimens XM-28c-3 and XM-28s-1 had more negative corrosion potentials at weeks 3 and 6, respectively, which do not correspond with increases in corrosion rate.

At the cathode (Figures 7a and 7b), the coiled and straightened XM-28 bars exhibited similar behavior, with corrosion potentials starting between -0.20 V and -0.25 V and becoming less negative throughout the test. After solution changes at 5 and 10 weeks, a drop in cathodic potential was observed for many specimens.

The average corrosion potentials for the XM-28s bars are comparable to those of the XM-28c bars (Figure 8). No significant differences between the anodic and cathodic potentials were observed for either coiled or straightened XM-28.

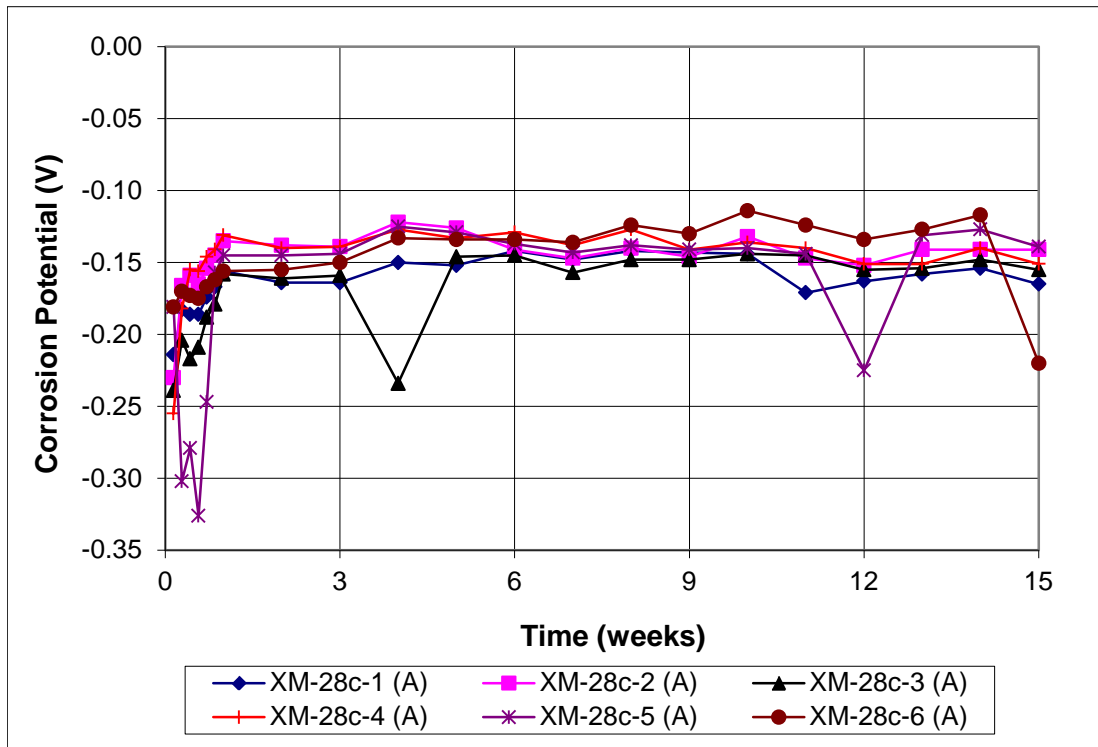


Figure 6a: Individual corrosion potentials (SCE) at anode for coiled XM-28 stainless steel from producer A.

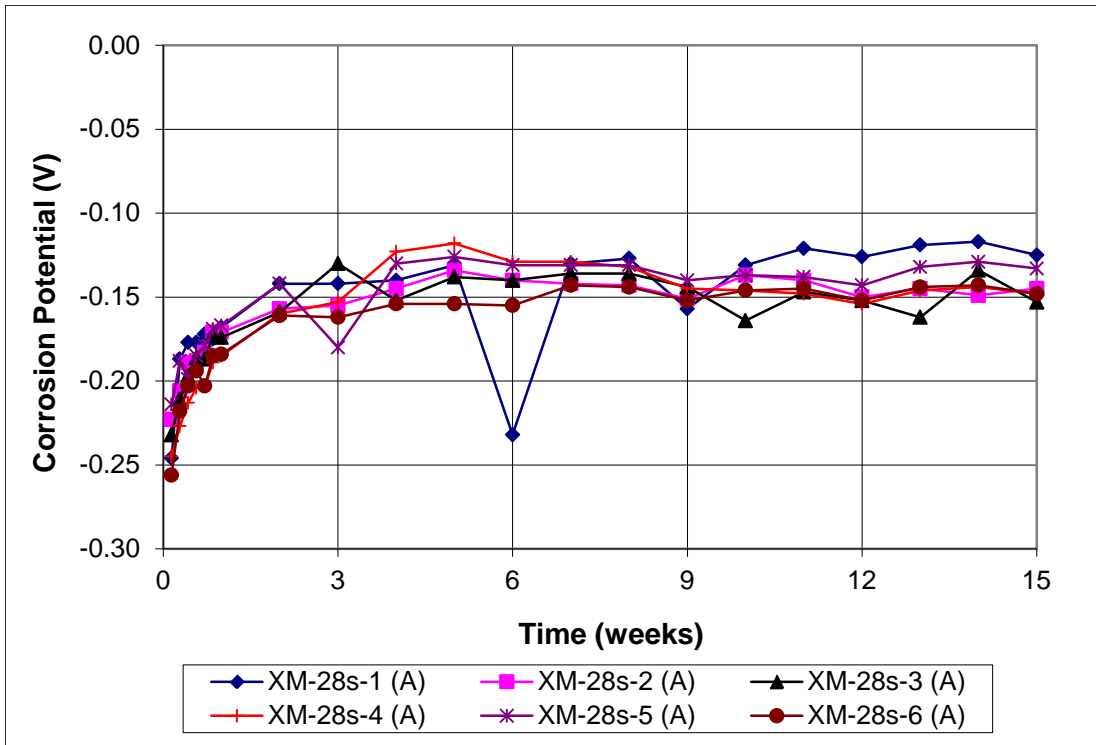


Figure 6b: Individual corrosion potentials (SCE) at anode for straightened XM-28 stainless steel from producer A.

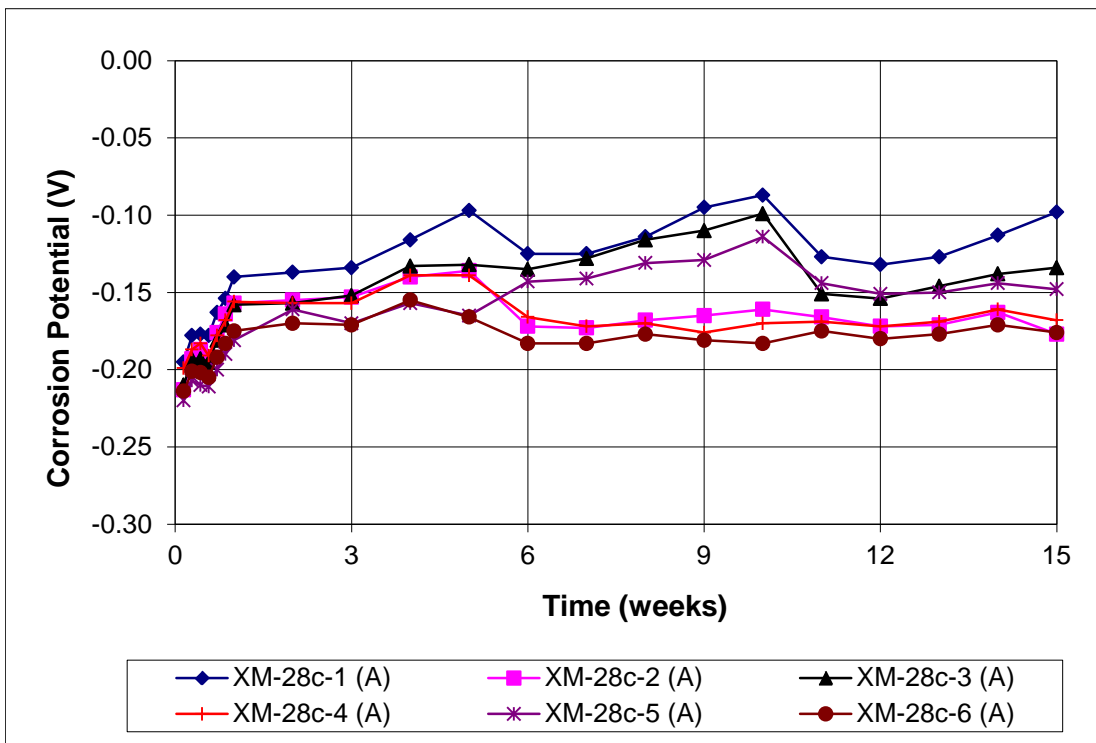


Figure 7a: Individual corrosion potentials (SCE) at cathode for coiled XM-28 stainless steel from producer A.

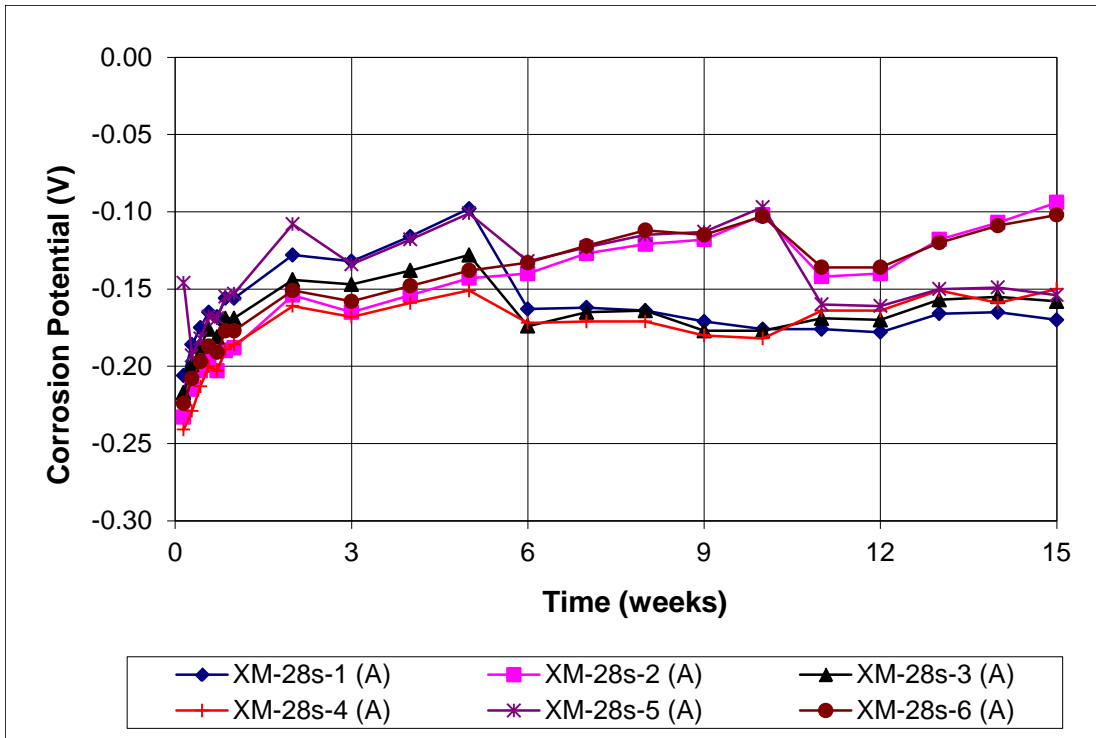


Figure 7b: Individual corrosion potentials (SCE) at cathode for straightened XM-28 stainless steel from producer A.

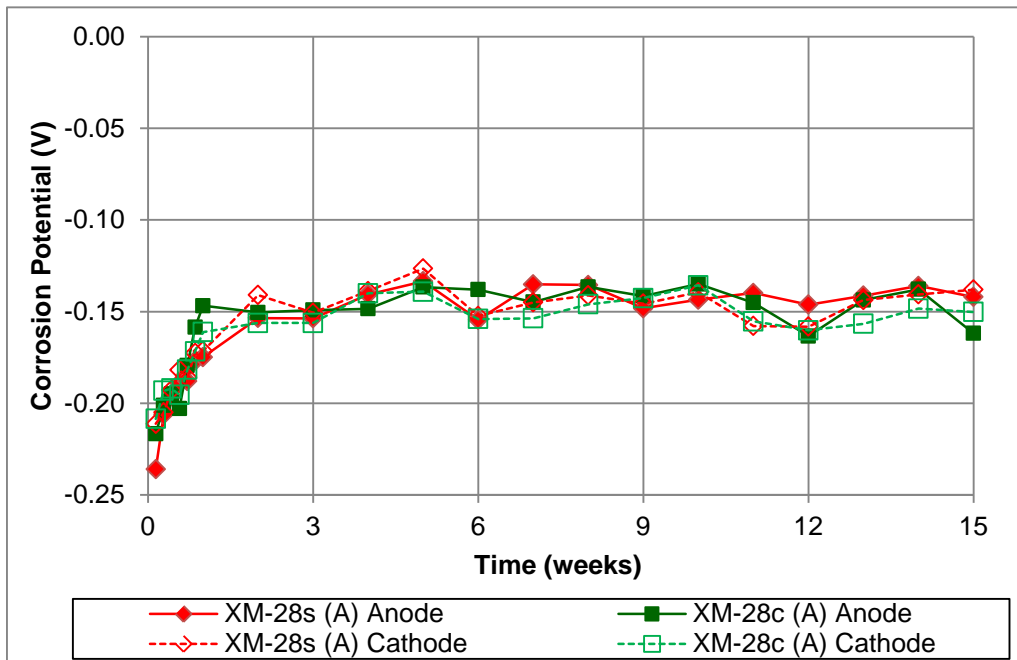


Figure 8: Average corrosion potentials (SCE) at anode for straightened (s) and coiled (c) XM-28 stainless steel from producer A.

The individual corrosion rates for the XM-28 and 2205 stainless steels from producer B are shown in Figures 9a and 9b, respectively. For XM-28 (Figure 9a), the corrosion rates for all specimens were zero or negative for the first three weeks of testing. The peak corrosion rate was 0.28 $\mu\text{m}/\text{yr}$ and occurred in specimen XM-28-3 at weeks 13 and 15. No specimen exceeded the 0.50 $\mu\text{m}/\text{yr}$ threshold in ASTM A955. For 2205 (Figure 9b), the corrosion rates for all specimens were negative for the first five days of testing. Specimen 2205-3 exceeded the 0.5 $\mu\text{m}/\text{yr}$ limit both before and after the week 5 solution change, as well as at weeks 6, 7, 9, 10, and weeks 12–15, reaching a peak corrosion rate of 5.71 $\mu\text{m}/\text{yr}$ at week 15. Specimen 2205-1 had a corrosion rate of 0.89 $\mu\text{m}/\text{yr}$ at week 6, and specimen 2205-5 had a corrosion rate of 0.55 $\mu\text{m}/\text{yr}$ at week 10. The three remaining specimens did not exceed the 0.50 $\mu\text{m}/\text{yr}$ threshold set in ASTM A955.

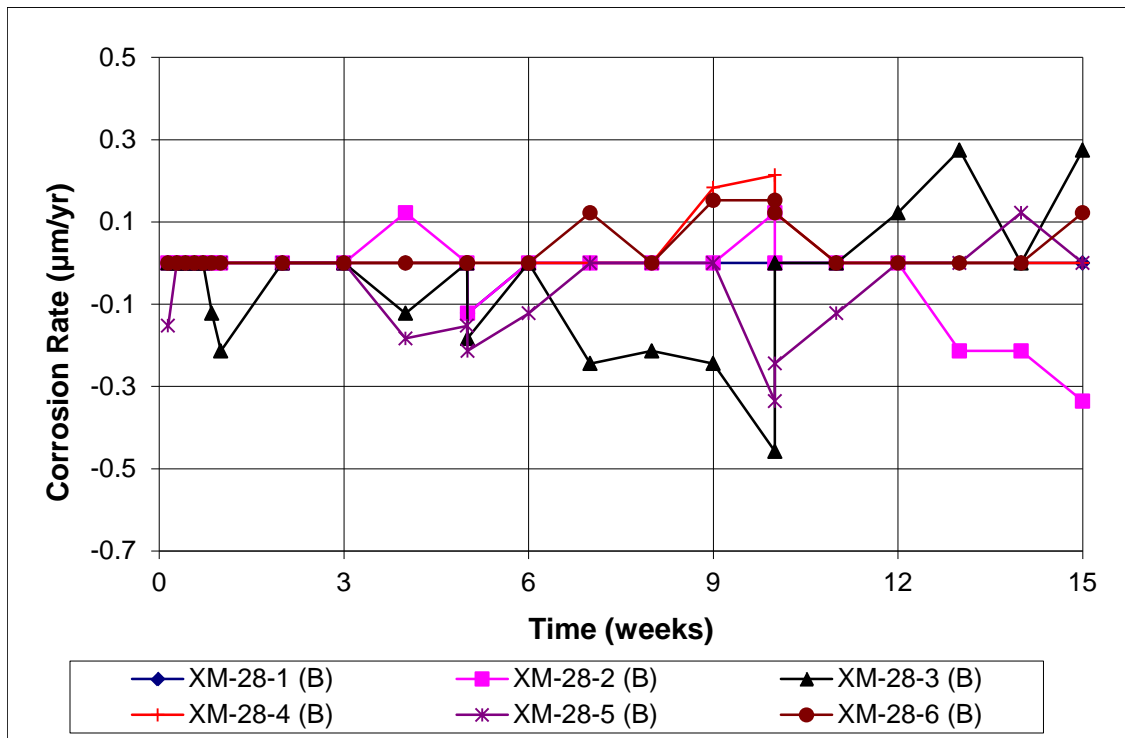


Figure 9a: Individual corrosion rates ($\mu\text{m}/\text{yr}$) for XM-28 stainless steel from producer B.

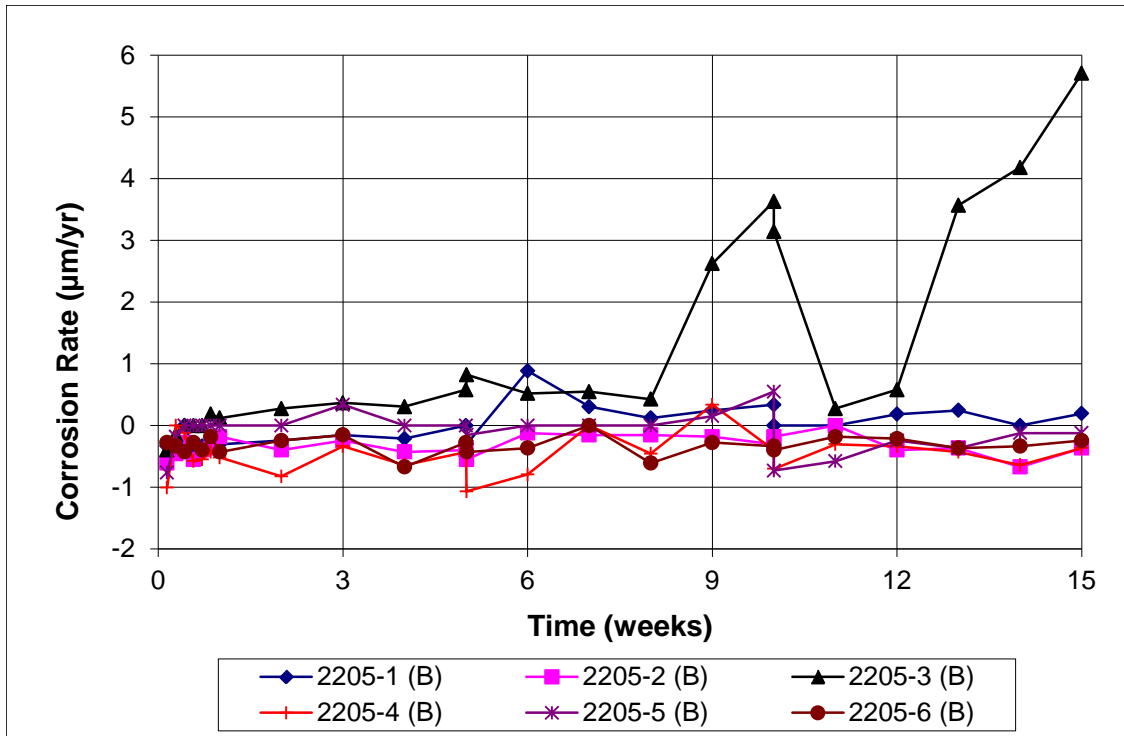


Figure 9b: Individual corrosion rates ($\mu\text{m/yr}$) for 2205 stainless steel from producer B.

The individual corrosion potentials at the anode are shown in Figures 10a and 10b for the XM-28 and 2205 bars, respectively. The individual cathode corrosion potentials are shown in Figures 11a and 11b. Average potentials are shown in Figure 12. Both XM-28 (Figure 10a) and 2205 (Figure 10b) bars have potentials between -0.11 V and -0.19 V at the start of testing. The corrosion potentials for the XM-28 bars became less negative over the first five weeks and then remained constant, approaching an average of -0.16 V for the duration of the test. The anode corrosion potentials of specimens 2205-2, 2205-5, and 2205-6 remained constant or became slightly more negative with time, while the anode potentials of specimens 2205-1, 2205-3, and 2205-4 showed significant drops in corrosion potential (Figure 10b) corresponding to increases in corrosion rate (Figure 9b).

The cathodic potential for the XM-28 bars from producer B (Figure 11a) remained near -0.15 V, with the exception of XM-28-4 and XM-28-6, which became less negative through the first ten weeks of testing. The cathodic potentials for specimens XM-28-4 and XM-28-6 were significantly less negative than the anodic potential from week 4 to week 10, corresponding with an increase in corrosion activity. Similar behavior was noted for the 2205 specimens; the cathode potentials for specimens 2205-1 and 2205-3 became less negative over time while the cathode potentials for the other specimens remained near -0.15 V (Figure 11b). The cathode potentials for specimens 2205-1 and 2205-3 were significantly less negative than their anodic potentials (Figure 10a). These specimens also exhibited the most positive corrosion rates during testing (Figure 9b).

The average corrosion potential for the 2205 bars was less negative than the average potential for XM-28 for both the first five and the last five weeks of testing, as shown in Figure 12. The average anodic and cathodic potentials for the two types of steel were similar throughout the test, with the exception of 2205 for weeks 8-10, where the average anodic potential was significantly more negative than the average cathodic potential.

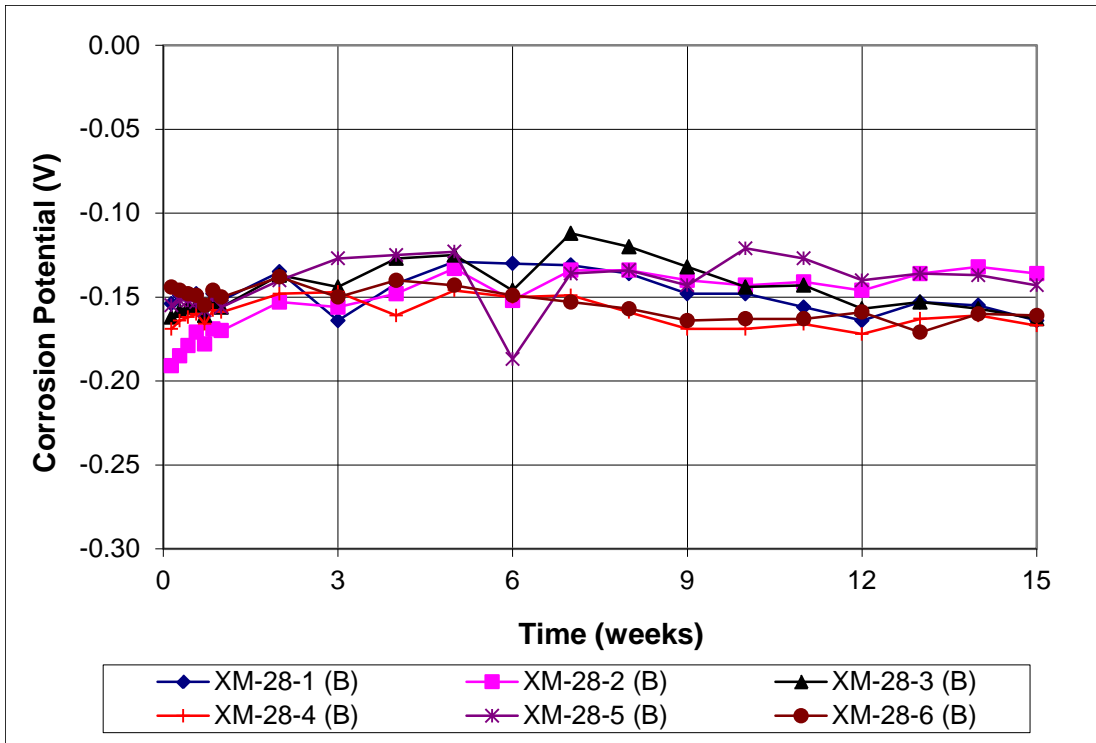


Figure 10a: Individual corrosion potentials (SCE) at anode for XM-28 stainless steel from producer B.

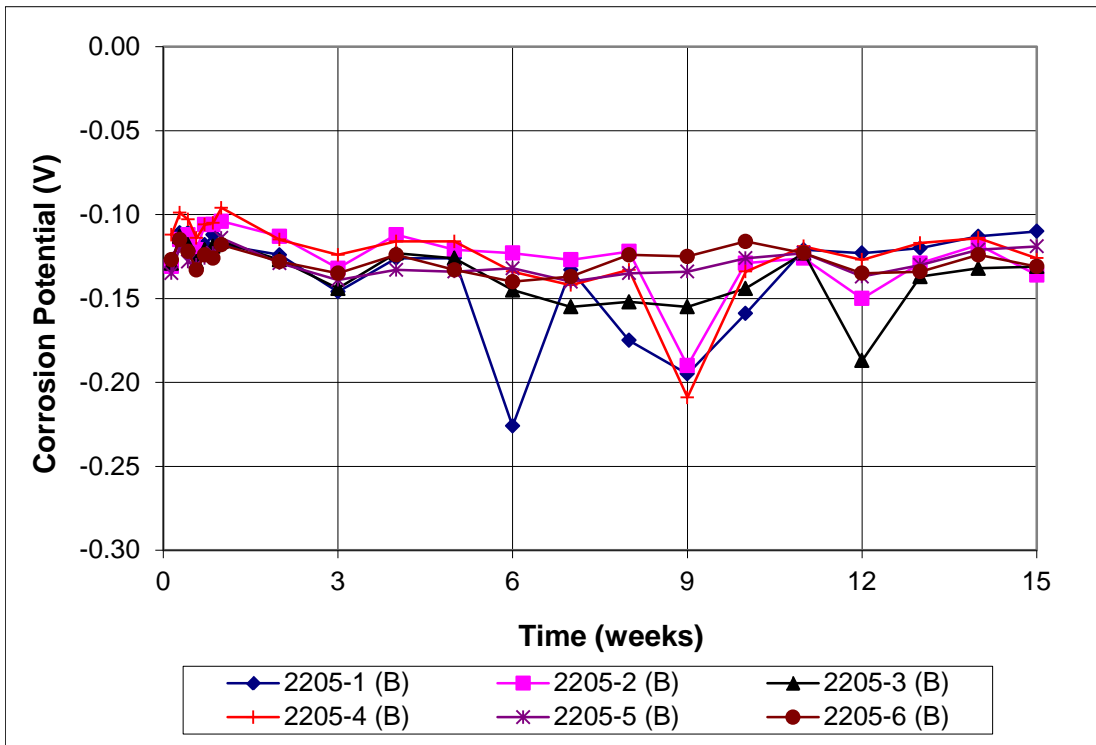


Figure 10b: Individual corrosion potentials (SCE) at anode for 2205 stainless steel from producer B.

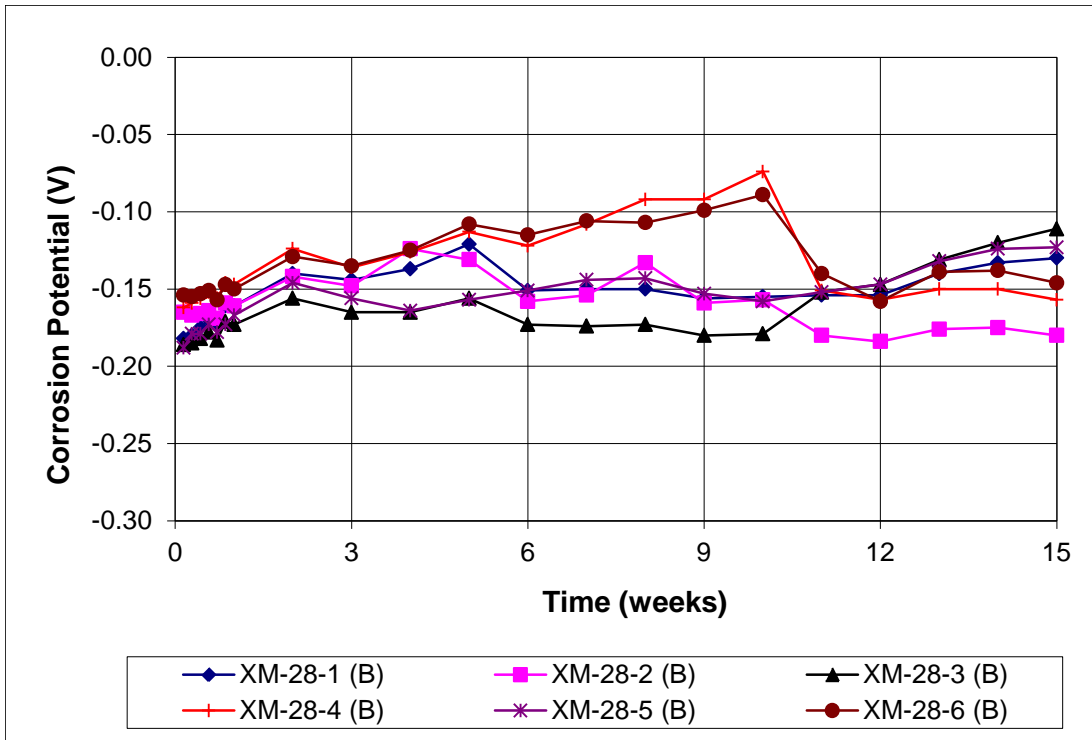


Figure 11a: Individual corrosion potentials (SCE) at cathode for XM-28 stainless steel from producer B.

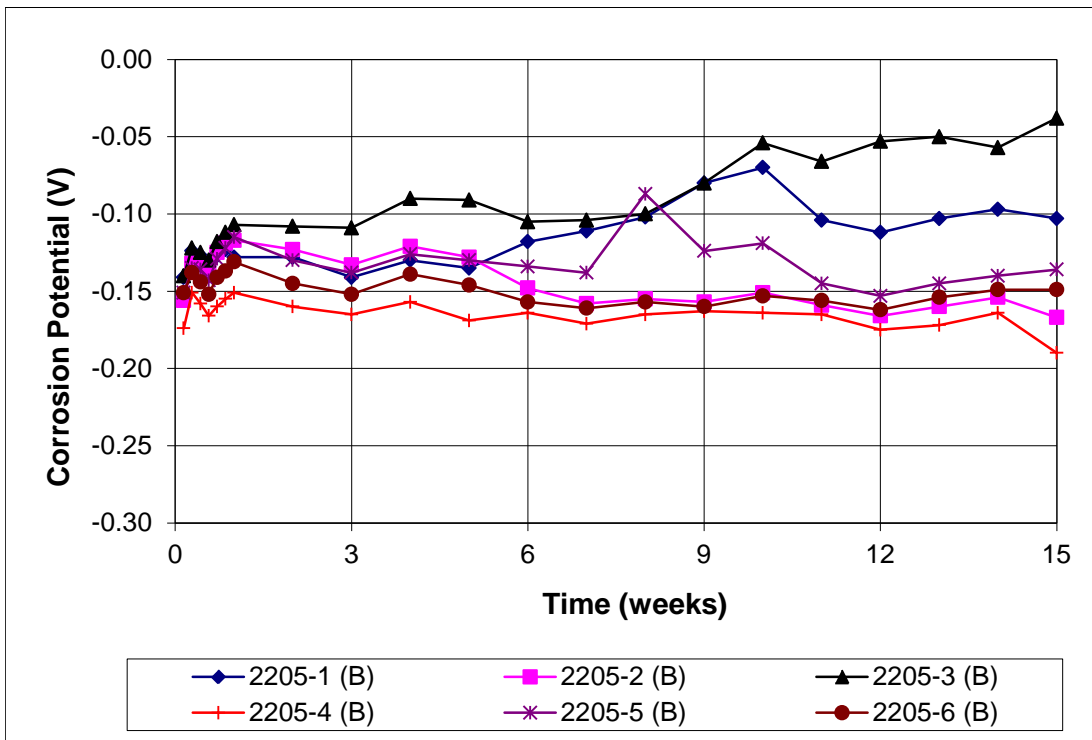


Figure 11b: Individual corrosion potentials (SCE) at cathode for 2205 stainless steel from producer B.

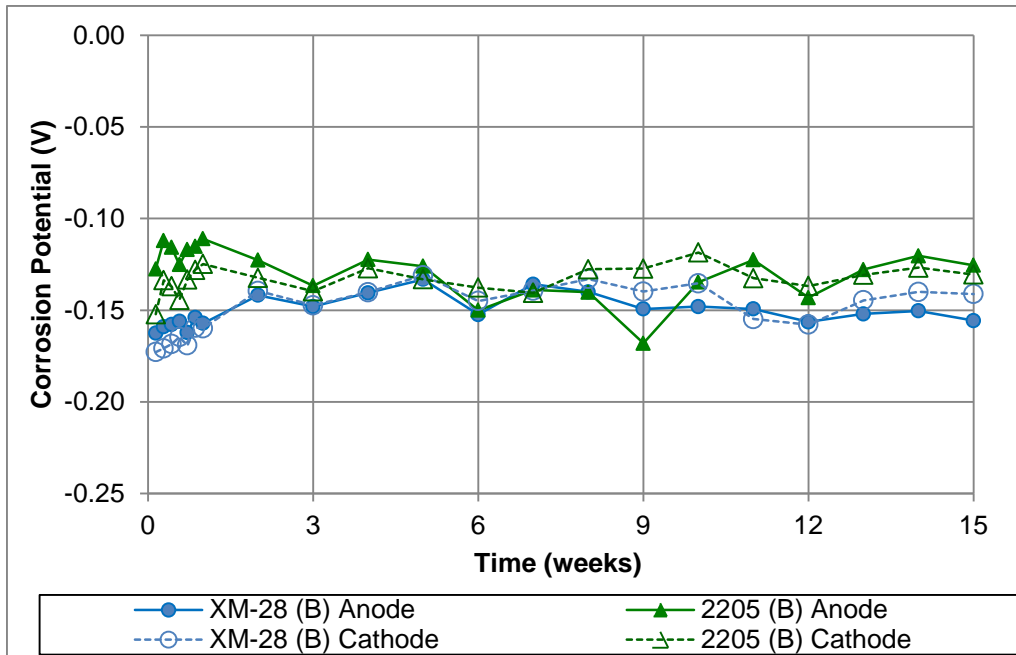


Figure 12: Average corrosion potentials (SCE) for XM-28 and 2205 stainless steels from producer B.

After testing, the bars were inspected for signs of corrosion. The coiled XM-28 from producer A showed no significant discoloration (Figure 13). Limited amounts of corrosion were observed on the anodes of specimens XM-28c-1 (Figure 14), XM-28c-3, and XM-28c-5. For these three specimens, corrosion products had formed on damaged areas of the transverse deformations. All straightened XM-28 bars from producer A showed moderate discoloration on both the anode and cathode after testing (Figure 15), with the exception of the anode of XM-28s-5 (Figures 16a and 16b), which showed severe discoloration at the anode but no discoloration at the cathode.



Figure 13: Coiled XM-28 stainless steel from producer A after testing; specimen XM28c-2. Anode (top bar) and cathode (bottom bars).



Figure 14: Coiled XM-28 stainless steel from producer A after testing; specimen XM28c-1. Anode bar with limited corrosion products at a damage site.



Figure 15: Straightened XM-28 stainless steel from producer A after testing; specimen XM28s-1. Anode (top bar) and cathode (bottom bars).



Figure 16a: Straightened XM-28 stainless steel from producer A after testing; specimen XM28s-5. Anode (top bar) and cathode (bottom bars).



Figure 16b: Straightened XM-28 stainless steel from producer A after testing; specimen XM28s-5. Anode bar with severe discoloration.

All of the XM-28 bars from producer B had some degree of discoloration. Specimen XM-28-5 showed the greatest degree of discoloration (Figure 17). Specimen XM-28-3 showed a similar degree of discoloration at the cathode. The remaining XM-28 specimens exhibited only very mild discoloration (Figure 18).



Figure 17: XM-28 stainless steel from producer B showing moderate discoloration after testing; specimen XM28-5. Anode (top bar) and cathode (bottom bars).



Figure 18: XM-28 stainless steel from producer B showing mild discoloration after testing; specimen XM28-1. Anode (top bar) and cathode (bottom bars).

All of the 2205 bars from producer B showed some degree of discoloration after testing (Figure 19a). Specimens 2205-1, 2205-4, and 2205-5 also had isolated corrosion products on the anode of the type shown in Figure 19b. Specimen 2205-3 had corrosion products over a moderate portion of the anode (Figures 20a and 20b). Specimens 2205-1, 2205-3, and 2205-5 all had a corrosion rate exceeding $0.5 \mu\text{m}/\text{yr}$ at some point during the test.



Figure 19a: 2205 stainless steel from producer B showing discoloration and corrosion products (arrow) after testing; specimen 2205-1. Anode (top bar) and cathode (bottom bars).



Figure 19b: 2205 stainless steel from producer B showing closeup of corrosion products (arrow) after testing; specimen 2205-1.



Figure 20a: 2205 stainless steel from producer B showing discoloration and corrosion products (arrow) after testing; specimen 2205-3. Anode (top bar) and cathode (bottom bars).



Figure 20b: 2205 stainless steel from producer B showing closeup of corrosion products after testing; specimen 2205-3.

SUMMARY AND CONCLUSIONS

The corrosion resistance of 2205 and XM-28 stainless steel bars from one of two producers and a single supplier was tested in accordance with Annexes A1 and A2 of ASTM 955-12e1. Three heats of stainless steel were tested: XM-28 stainless steel from producer A, 2205 stainless steel from producer B, and XM-28 stainless steel, also from producer B. The bars from producer A were supplied in two conditions, as cut from the coil and after having been straightened, while the bars supplied by producer B were rolled straight.

The following conclusions are based on the test results presented in this report:

- 1) The XM-28 stainless steel bars tested in this study satisfied the requirements specified in Annexes A1 and A2 of ASTM 955.
- 2) The 2205 stainless steel bars tested in this study did not satisfy the requirements specified in Annexes A1 and A2 of ASTM 955, exhibiting individual corrosion rates greater than 0.50 $\mu\text{m}/\text{yr}$ and an average corrosion rate greater than 0.25 $\mu\text{m}/\text{yr}$.
- 3) The process of straightening coiled stainless steel reinforcement damages the transverse deformations of the bars and can leave deposits, either of which can serve as initiation sites for corrosion. The two forms of XM-28 bars from producer A, however, exhibited no significant difference in macrocell corrosion rate.

REFERENCES

ASTM A955, 2012, “Standard Specification for Plain and Deformed Stainless-Steel Bars for Concrete Reinforcement (ASTM A955/A955M-12e1),” ASTM International, West Conshohocken, PA, 11 pp.

ASTM C876, 2009, “Standard Test Method for Corrosion Potentials of Uncoated Reinforcing Steel in Concrete (ASTM C876-09),” ASTM International, West Conshohocken, PA, 7 pp.